GEODESIC REGRESSION OF IMAGE AND SHAPE DATA FOR IMPROVED MODELING OF 4D TRAJECTORIES

James Fishbaugh[1], Marcel Prastawa[1], Guido Gerig[1], Stanley Durrleman[2]*

[1]Scientific Computing and Imaging Institute, University of Utah

[2]INRIA/ICM, Pitié Salpêtrière Hospital, Paris, France

ABSTRACT

A variety of regression schemes have been proposed on images or shapes, although available methods do not handle them jointly. In this paper, we present a framework for joint image and shape regression which incorporates images as well as anatomical shape information in a consistent manner. Evolution is described by a generative model that is the analog of linear regression, which is fully characterized by baseline images and shapes (intercept) and initial momenta vectors (slope). Further, our framework adopts a control point parameterization of deformations, where the dimensionality of the deformation is determined by the complexity of anatomical changes in time rather than the sampling of the image and/or the geometric data. We derive a gradient descent algorithm which simultaneously estimates baseline images and shapes, location of control points, and momenta. Experiments on real medical data demonstrate that our framework effectively combines image and shape information, resulting in improved modeling of 4D (3D space + time) trajectories.

1. INTRODUCTION

Analysis of longitudinal data incorporating both spatial and temporal information is essential for various clinical tasks such as predicting patient outcome and measuring efficacy of different therapeutic strategies. A crucial tool for longitudinal analysis is regression of observed data, which enables interpolation to generate continuous evolution models as well as extrapolation to predict future observations. Regression models are also necessary for conducting population studies comparing the change trajectories of different subjects.

In medical imaging, it is important to consider image data in anatomical context, which motivates regression on image and shape data in different combinations (a multi-object complex). A variety of regression schemes have been proposed on images or shapes, although available methods do not handle them jointly. For example, the extension of kernel regression for image data [1] or piecewise linear regression for time series of images [2] and shapes [3]. Combining intensity and geometric information has been explored for registration [4].

To conduct statistical analysis on 4D (3D space + time) data, it is particularly useful to consider compact generative regression models which have low number of parameters situated at only one chosen time point. Geodesic regression is such a model and is fully characterized by baseline images and shapes (the intercept) and the tangent vector defining the geodesic at the baseline objects (the slope). Geodesic regression frameworks for images [5, 6] and for shapes [7] have been proposed using the LDDMM setting. However, no notion of how to combine images and shape data is provided.

We propose a novel geodesic regression framework that leverages image and shape data together to estimate a single deformation of the ambient space. We use the currents representation for geometric data that allows flexible representation of a wide variety of shape objects such as point sets, curves, or surface meshes, without the need for point correspondence between shapes. Compared to image regression alone, shape data provides anatomical information that constrains the regression, especially in cases where images have low contrast, by placing larger weights on regions with anatomical importance. Compared to shape regression alone, image information provides data in areas where segmentations are not available, as well as providing context to regions surrounding anatomical objects. Our framework uses the control-point parameterization of geodesic flows introduced in [8], which makes the parameterization of the deformation independent from the data. This allows us to keep a reasonable dimension of the parameterization, which is determined by the complexity of anatomical changes in time, and not the sampling of the data. We therefore combine image and shape data without introducing a complexity overhead.

2. METHODOLOGY

We perform regression on observed time-series data of images I_i and shapes X_i, each acquired at time-point t_i. Shape data may consist of a mix of point sets, curves, or surface meshes where all vertices are concatenated into one vector X_i.

[*]Supported by grants: RO1 HD055741 (ACE, project IBIS), U54 EB005149 (NA-MIC), and U01 NS082086 (HD) and the Utah Science Technology and Research (USTAR) initiative at the University of Utah.

978-1-4673-1961-4/14/$31.00 ©2014 IEEE

We use the control point formulation of [8] to generate geodesic flows of diffeomorphisms. Let $\mathbf{S}_0 = \{c_{0,k}, \alpha_{0,k}\}$ be a set of momentum vectors $\alpha_{0,k}$ attached to control points $c_{0,k}$ distributed in the image domain. Geodesic flows are computed by evolving control points and momenta by integrating the following Hamiltonian equations over the time interval of interest:

$$\begin{cases} \dot{c}_k(t) = \sum_{i=1}^{N} K(c_k(t), c_i(t))\alpha_i(t) \\ \dot{\alpha}_k(t) = -\sum_{i=1}^{N} \alpha_k(t)^T \alpha_i(t) \nabla_1 K(c_k(t), c_i(t)) \end{cases} \quad (1)$$

with initial conditions $c_k(0) = c_{0,k}$ and $\alpha_k(0) = \alpha_{0,k}$ (assuming starting time-point to be 0), and K is a Gaussian kernel with variance σ_V^2 which controls the spatial scale of deformation. For simplicity, we write these equations as $\dot{\mathbf{S}}(t) = F(\mathbf{S}(t))$ with $\mathbf{S}(0) = \mathbf{S}_0$. The convolution of the momenta defines the following time-varying velocity field: $v(t,x) = \sum_{i=1}^{N} K(x, c_i(t))\alpha_i(t)$ for any point x in the domain. The velocity is used to deform the domain: a particle at point x at time 0 moves to $\phi(t,x)$ at later time t, where $\phi(t,x)$ follows the integral curve of $\frac{\partial \phi(t,x)}{\partial t} = v(t, \phi(t,x))$ starting with $\phi(0,x) = x$. In this formulation, the velocity of the particle is given by the field $v(t,.)$ at its current location. It has been shown in [9] that for all t, $\phi(t,.)$ is a 3D diffeomorphism.

Following this model, the vertices of a given baseline shape complex concatenated into a vector X_0 move at time t to $X(t) = \phi(t, X_0)$, which satisfies the ordinary differential equation (ODE): $\dot{X}(t) = v(t, X(t))$ with $X(0) = X_0$. To make explicit the dependency of the equation of motion on $\mathbf{S}(t)$, we write it as: $\dot{X}(t) = G(X(t), \mathbf{S}(t))$.

A given baseline image I_0 is also deformed by the flow of diffeomorphisms and its trajectory is given as $I(t) = I_0 \circ \phi(t,.)^{-1}$. The inverse flow satisfies the equation $\frac{\partial \phi(t,.)^{-1}}{\partial t} = -d\phi(t,.)^{-1} v(t,.)$. For the sake of simplicity, we denote $Y(t,.) = \phi(t,.)^{-1}$, a L^2 function that maps the point x to its position at time t under the inverse flow $\phi^{-1}(t,x)$. This maps satisfies $\dot{Y}(t,.) = -dY(t,.)v(t,.) = H(Y(t,.), \mathbf{S}(t))$, where we make explicit the dependency on $\mathbf{S}(t)$. At time t, the intensity of the warped baseline image at voxel position x is given by $I(t,x) = I_0(Y(t,x))$ using 3D interpolation.

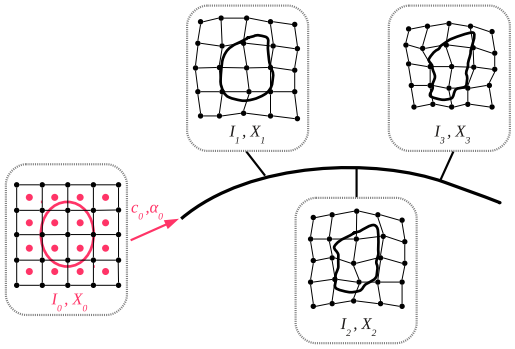

Fig. 1. Conceptual overview of geodesic regression on multi-object complexes containing both image and shape data. The framework estimates parameters at $t = 0$ which consist of the baseline image I_0 and shape X_0 along with the deformation model parameterized by control points c_0 and initial momenta α_0 such that overall distance between the deformed objects and the observations are minimal.

A conceptual overview of our framework is shown in Fig. 1 where regression is performed by minimizing the overall distance between the observations and the deformed baseline objects (shapes and/or images). Let $d(X(t_i), X_i)$ be a metric between the deformed baseline shape complex X_0 at time t_i and the data shape complex X_i. This metric may be a weighted sum over each component of the shape complex of the currents metric between sets of curves or surface meshes. This term essentially depends on $X(t_i)$ and is denoted $A(X(t_i))$. Similarly, we have a metric $d(I(t_i), I_i)$ denoted as $B(Y(t_i,.))$ that is the sum of squared differences between the deformed baseline image $I_0 \circ Y(t_i,.)$ and the observed image I_i.

The geodesic regression problem amounts to finding the deformation parameters $\mathbf{S}_0$ and baseline anatomical configuration (I_0, X_0) such that the following criterion is minimized:

$$E(\mathbf{S}_0, I_0, X_0) = \sum_{t_i} \left(\lambda_{I_{t_i}} A(X(t_i)) + \lambda_{S_{t_i}} B(Y(t_i,.)) \right) + L(\mathbf{S}_0) \quad (2)$$

subject to

$$\begin{cases} \dot{\mathbf{S}}(t) = F(\mathbf{S}(t)) & \mathbf{S}(0) = \mathbf{S}_0 \\ \dot{X}(t) = G(X(t), \mathbf{S}(t)) & X(0) = X_0 \\ \dot{Y}(t,.) = H(Y(t,.), \mathbf{S}(t)) & Y(0,.) = \mathrm{Id} \end{cases} \quad (3)$$

where the regularizer $L(\mathbf{S}_0) = \sum_{i,j=1}^{N} \alpha_{0,i}^T K(c_{0,i}, c_{0,j}) \alpha_{0,j}$ is the squared norm of initial velocity and weights on image and shape matching $\lambda_{I_{t_i}}$ and $\lambda_{S_{t_i}}$.

As shown in the supplemental material (`www.cs.utah.edu/~jfishbau/docs/isbi2014_eqns.pdf`), the gradient is computed by integrating 3 linear ODEs with source terms from final time-point T_f back to time-point 0:

$$\nabla_{\mathbf{S}_0} E = \xi(0) + \nabla_{\mathbf{S}_0} L \qquad \nabla_{X_0} E = \eta(0)$$
$$\frac{1}{2} \nabla_{I_0} E = \sum_{t_j} \mathrm{Splat}_{Y(t_j,.)}(I_0 \circ Y(t_j,.) - I_i)$$

with

$$\begin{cases} \dot{\eta}(t) = -\partial_1 G(t)^T \eta(t) - \sum_{t_i} \nabla_{X(t_i)} A \, \delta(t - t_i) \\ \dot{\theta}(t) = -\partial_1 H(t)^\dagger \theta(t) - \sum_{t_i} \nabla_{Y(t_i,.)} B \, \delta(t - t_i) \\ \dot{\xi}(t) = -\partial_2 G(t)^T \eta(t) - \partial_2 H(t)^\dagger \theta(t) - d_{\mathbf{S}(t)} F^T \xi(t) \end{cases}$$

with final conditions $\eta(T_f) = \theta(T_f) = \xi(T_f) = 0$.

The vector η is same size as X_0, which brings back to time $t = 0$ the gradients of the data matching terms, and is used to update the position of the vertices of the baseline shape complex. Similarly θ is of the same size as $Y(0, .)$ (an image of vectors in practice) which integrates the successive gradients of the image matching terms that acts as jumps in the differential equation. Finally, ξ is a variable of the same size as $\mathbf{S}_0$ which is used at time $t = 0$ to update the deformation parameters (the position of the control points and their momentum vectors). The gradient with respect to the baseline image involves the splatting of the current residual images at positions $Y(t_i, .)$ as done in [8].

3. RESULTS AND DISCUSSION

Pediatric Brain Development: We explore the impact of joint image and shape regression in modeling pediatric brain development. The data consists of T1W images of the *same* healthy child observed at 6, 12, and 25 months of age. Regression on images alone is difficult in this case due to the very low contrast in the 6 month old image. Despite the low contrast, tissue segmentations can still be reliably and consistently estimated [10]. We estimate a geodesic model using only T1W images and a model jointly on images and white matter surfaces to emphasize the development of the tissue interface. We initialize 120 control points on a regular grid with the deformation kernel $\sigma_V = 20$ mm. Finally, due to limited contrast at 6 months, we estimate the baseline at 25 months and follow the evolution backwards in time.

The results of geodesic regression are shown for several snapshots in time in Fig. 2. The model estimated using only images mostly captures the scale change, but does not capture much deformation in the interior of the brain. The model estimated jointly on image and shape captures more detailed development as white matter stretches and expands.

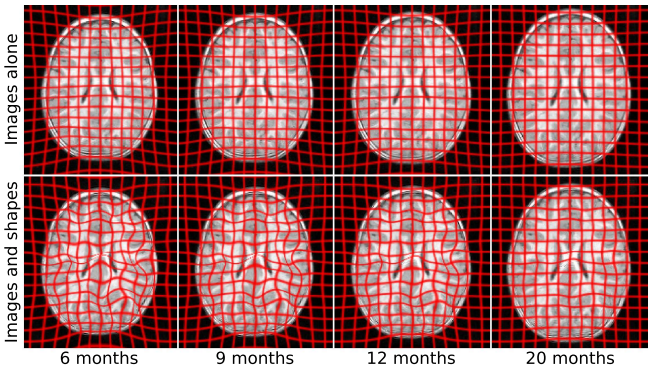

Fig. 2. Images and deformations estimated by geodesic regression using images alone (top) and jointly on images and white matter surfaces (bottom). Regression jointly on image and shape results in a more realistic evolution which captures detailed changes in brain tissue in addition to the increase in brain size. In both cases, geodesic regression was estimated backwards in time.

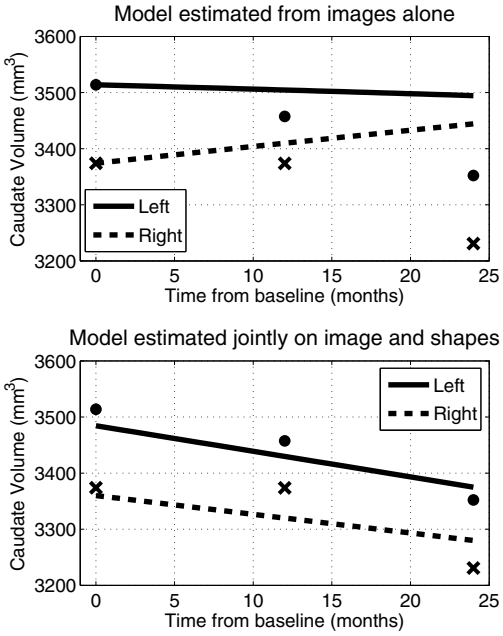

Fig. 3. Caudate volume extracted continuously after regression compared to observed caudate volumes (circles and x's). Volume is measured continuously from the modeled shape trajectories, not fitted to discrete volume measurements. The model estimated on images alone fails to capture the volume loss. Evolution of caudates for the image only model is *not* estimated, but instead we shoot the baseline caudate shapes along the geodesic estimated from images alone. Note: measurements extracted continuously from non-linearly deforming shapes can produce either linear or non-linear trends with no prior assumption of linearity.

Neurodegeneration in Huntington's Disease: Next, we investigate the application of joint image and shape regression to Huntington's disease (HD) where accurate 4D models are needed to measure the effectiveness of therapies or drug treatments. In HD, degeneration of the caudate has been shown to be significant [11]. Here we explore T1W image data from a single patient diagnosed with HD scanned at 58, 59, and 60 years of age. Sub-cortical structures are segmented, manually verified, and cleaned. Models are estimated using only T1W images as well as T1W images plus caudate surfaces. Control points are initialized on a regular grid with 10 mm spacing with kernel $\sigma_V = 10$ mm.

The trajectory of caudate volume extracted *after* regression is shown in Fig. 3. The model estimated from images alone fails to capture the volume loss observed in both caudates, and rather, shows an increase in right caudate volume. By incorporating caudate shape data in model estimation, we

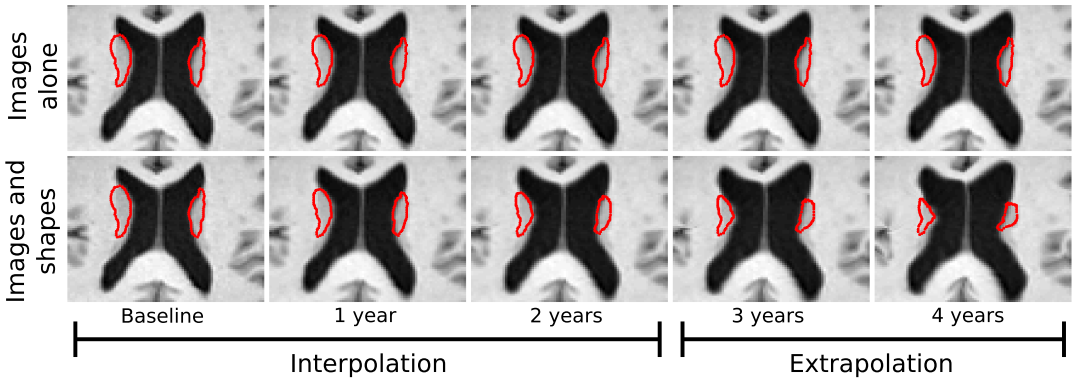

Fig. 4. **Top)** Evolution estimated on images alone. Evolution of caudates are *not* estimated, but instead we shoot the baseline caudate shapes along the estimated geodesic. **Bottom)** Evolution estimated jointly using images and caudate shapes. Regression on images alone results in a slight expansion of ventricles, but does not capture the shrinking of caudates. Our method is able to capture both the expansion of ventricles and the shrinking of caudates.

are able to capture the shrinking of the caudates. The corresponding expansion of the ventricles is also captured, shown in Fig 4, due to the inclusion of imaging data. By incorporating shape and image information jointly, we are able to model both the expansion of the ventricles and the degeneration of the caudates. Accurate models of change are essential when extrapolating beyond the observation time interval, which can provide insight into disease progression.

Conclusions: We presented a novel geodesic regression framework that jointly considers image and shape information in the LDDMM framework, where dense diffeomorphisms are built using a control point formulation. This formulation decouples deformation parameters from input object parameters (e.g., voxels, surface points) providing greater flexibility and consistency in mapping different object types across time. Our regression model seamlessly handles images and multi-object complexes consisting of points, curves, and/or surfaces in different combinations. Experiments show that our framework effectively combines image and shape information to estimate a single deformation of the ambient space, resulting in improved modeling of 4D trajectories.

4. REFERENCES

[1] B.C. Davis, P.T. Fletcher, E. Bullitt, and S. Joshi, "Population shape regression from random design data," in *ICCV*. 2007, pp. 1–7, IEEE.

[2] A.R. Khan and M.F. Beg, "Representation of time-varying shapes in the large deformation diffeomorphic framework," in *ISBI*. 2008, pp. 1521–1524, IEEE.

[3] S. Durrleman, X. Pennec, A. Trouvé, J. Braga, G. Gerig, and N. Ayache, "Toward a comprehensive framework for the spatiotemporal statistical analysis of longitudinal shape data," *IJCV*, pp. 1–38, 2012.

[4] P. Cachier, E. Bardinet, D. Dormont, X. Pennec, and N. Ayache, "Iconic feature based nonrigid registration: the pasha algorithm.," *Computer Vision and Image Understanding*, vol. 89, no. 2-3, pp. 272–298, 2003.

[5] M. Niethammer, Y. Huang, and F.X. Vialard, "Geodesic regression for image time-series," in *MICCAI*, 2011, vol. 6892 of *LNCS*, pp. 655–662.

[6] N.P. Singh, J. Hinkle, S. Joshi, and P.T. Fletcher, "A vector momenta formulation of diffeomorphisms for improved geodesic regression and atlas construction," in *ISBI*, 2013, pp. 1219–1222.

[7] J. Fishbaugh, M. Prastawa, G. Gerig, and S. Durrleman, "Geodesic shape regression in the framework of currents," in *IPMI*, 2013, vol. 23, pp. 718–729.

[8] S. Durrleman, M. Prastawa, G. Gerig, and S. Joshi, "Optimal data-driven sparse parameterization of diffeomorphisms for population analysis," in *IPMI*, 2011, vol. 6801 of *LNCS*, pp. 123–134.

[9] S. Joshi and M. Miller, "Landmark matching via large deformation diffeomorphisms," *IEEE Trans. Image Processing*, vol. 9, no. 8, pp. 1357–1370, 2000.

[10] A. Vardhan, M. Prastawa, S. Gouttard, J. Piven, and G. Gerig, "Quantifying regional growth patterns through longitudinal analysis of distances between multimodal MR intensity distributions," in *ISBI*, 2012, pp. 1156–1159.

[11] EH. Aylward, AM. Codori, A. Rosenblatt, M. Sherr, J. Brandt, OC. Stine, PE. Barta, GD. Pearlson, and CA. Ross, "Rate of caudate atrophy in presymptomatic and symptomatic stages of huntington's disease," *Movement Disorders*, vol. 15, no. 3, pp. 552–560, 2000.